

**Kinetics of volume and enthalpy relaxation in Pt<sub>60</sub>Ni<sub>15</sub>P<sub>25</sub> bulk metallic glass**M. Kohda,<sup>1</sup> O. Haruyama,<sup>1</sup> T. Ohkubo,<sup>2</sup> and T. Egami<sup>3,4,5</sup><sup>1</sup>*Department of Physics, Faculty of Science and Technology, Tokyo University of Science, Noda 278-8510, Japan*<sup>2</sup>*National Institute for Materials Science, Tsukuba 305-0047, Japan*<sup>3</sup>*Department of Material Science and Engineering, University of Tennessee, Knoxville, Tennessee 37996, USA*<sup>4</sup>*Department of Physics and Astronomy, University of Tennessee, Knoxville, Tennessee 37996, USA*<sup>5</sup>*Oak Ridge National Laboratory, Oak Ridge, Tennessee 37831, USA*

(Received 5 February 2009; published 17 March 2010)

We examined the kinetics of the structural relaxation in a Pt<sub>60</sub>Ni<sub>15</sub>P<sub>25</sub> bulk metallic glass by density and enthalpy measurements. Measurements were made slightly below the glass transition temperature, with and without preannealing at a temperature above the glass transition temperature. The results are elucidated in terms of the two-components model, which includes positive as well as negative fluctuations in local density.

DOI: 10.1103/PhysRevB.81.092203

PACS number(s): 61.43.Fs, 65.60.+a, 61.20.Lc

Metallic glasses show some superior physical properties which make them promising for industrial applications, particularly after the recent development of bulk metallic glasses (BMGs).<sup>1,2</sup> However, just as any glasses,<sup>3</sup> they show considerable structural relaxation,<sup>4,5</sup> and understanding and controlling the relaxation remains one of the challenges. The structural relaxation in metallic glasses has been investigated by diffraction<sup>6</sup> and other techniques but the recent development of BMG allowed the investigation over wider ranges of temperature and time. Recent studies of structural relaxations in BMG include the studies of viscosity,<sup>7,8</sup> positron annihilation,<sup>9</sup> enthalpy,<sup>10</sup> and physical density.<sup>11</sup>

The kinetics of structural relaxation is usually described by a stretched exponential relaxation function,

$$P(t) = P_{as} + (P_{eq} - P_{as})\{1 - \exp[-(t/\tau)^\beta]\}, \quad (1)$$

where  $\tau$  is relaxation time and  $\beta$  is Kohlrausch exponent. Busch *et al.*<sup>8</sup> reported viscosity data for Zr<sub>46.75</sub>Ti<sub>8.25</sub>Cu<sub>7.5</sub>Ni<sub>10</sub>Be<sub>27.5</sub> BMG in a sub- $T_g$  region and fitted data to Eq. (1) with  $\beta$  of about 0.8. Haruyama *et al.*<sup>11</sup> performed the density relaxation experiment for Pd<sub>40</sub>Ni<sub>40</sub>P<sub>20</sub> BMG in a sub- $T_g$  region and showed that its relaxation process was well described by Eq. (1) with  $\beta$  of about 0.66. However, the process of structural relaxation is complex, depending on the fictive temperature in a nontrivial way.<sup>3</sup> Whereas the relaxation in metallic glasses is often described in terms of the free-volume model,<sup>12–14</sup> the validity of applying the free-volume model to metallic system was questioned from the beginning.<sup>12</sup> The difficulties of the free-volume model to explain diffusion are also well documented.<sup>15</sup> In this Brief Report, we demonstrate that at least two components are needed to explain the results, and suggest that the local-density-fluctuation model provides a better description of the phenomenon.

To prepare samples, the molten Pt<sub>60</sub>Ni<sub>15</sub>P<sub>25</sub> alloy was water quenched into room temperature from  $T=923$  K (40 K above liquidus temperature) and the bulk glass with a size of 6 or 8 mm in diameter and 10 mm in length were fabricated.<sup>11</sup> The amorphous nature of the glass was checked by x-ray diffraction. The apparent glass transition temperature is determined as  $T_g=476$  K by differential scanning calorimetry (DSC) at a heating rate of 0.167 K/s. The measurements of physical density were performed at room

temperature after relaxing the bulk samples at 461 K ( $T_g-15$  K) for various periods of time. The details of density measurement are reported elsewhere.<sup>11</sup> The enthalpy relaxation was investigated by measuring the specific heat of samples annealed at 461 K for different times with a Perkin-Elmer Pyris1 DSC conducted at a heating rate of 0.167 K/s. During isothermal annealing at 461 K, the sample relaxes toward a state with lower enthalpy because of structural relaxation. After the relaxation measurement, the sample is heated in the DSC apparatus and then the enthalpy lost during relaxation was evaluated by measuring the enthalpy to reach the supercooled liquid state above  $T_g$ . The preannealed samples were prepared by annealing the as-quenched samples at 506 K ( $T_g+30$  K) in the supercooled liquid region. It is verified by density measurement that the fully relaxed state was achieved by annealing at 506 K for 480 s.<sup>11</sup> The density decreased from  $d_{as}=15.3616 \pm 0.0005$  to  $15.3593 \pm 0.0005$  g/cm<sup>3</sup> after the relaxation. This decrease in density indicates that the preannealing temperature (506 K) was higher than the fictive temperature of the as-cast glass. High-resolution transmission electron microscopy (HRTEM) image of relaxed sample was taken with a FEI Tecnai G2 F30 U-TWIN operated at 300 keV, where the sample was thinned by ion milling at about 100 K.

Figure 1 shows the change in the specific volume,  $v(t)$ , of as-quenched and preannealed Pt<sub>60</sub>Ni<sub>15</sub>P<sub>25</sub> BMGs, relaxed at 461 K, 15 K below  $T_g$ , for time  $t$  and measured at room temperature. The kinetics of the preannealed sample is faster than that of the as-cast sample, again consistent with the observation that the fictive temperature of the as-cast sample is lower than 506 K. Both, however, reach the same final state, as expected. The inset of Fig. 1 shows the x-ray diffraction pattern before and after the relaxation to prove no crystallization occurred during the measurement.

Figure 2(a) shows the DSC curves of the as-quenched Pt<sub>60</sub>Ni<sub>15</sub>P<sub>25</sub> BMG samples after annealing at 461 K for different annealing times, listed in figure. It can be seen that the temperature of crystallization onset and the crystallization enthalpy show little change up to the annealing time as long as  $4.8 \times 10^4$  s. The enthalpy recovery during the glass transition is equal to the enthalpy difference,  $\Delta H_g(t) = H_l - H_g(t)$ , between the relaxed glass and the liquid state, where  $H_l$  is the enthalpy in a supercooled liquid state and  $H_g(t)$  corresponds to the enthalpy of the sample relaxed for

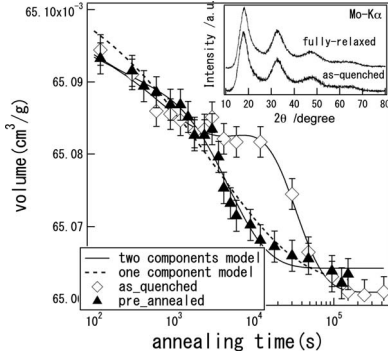


FIG. 1. Room-temperature-specific volume of  $\text{Pt}_{60}\text{Ni}_{15}\text{P}_{25}$  BMG,  $v(t)$ , as a function of annealing time for 461 K (15 K below  $T_g$ ) in the as-quenched and preannealed samples. The inset presents the x-ray diffraction profiles for samples in the as-quenched and relaxed states. Solid lines illustrate the calculations by Eq. (2) (see text).

time  $t$ . The enthalpy difference was evaluated by integrating the specific-heat curve from 461 to 515 K in the supercooled liquid region. Figure 2(b) shows the plot of the enthalpy change,  $\Delta H_g(t) = \Delta H_{lg}(t) - \Delta H_{lg}(120) = H_g(120) - H_g(t)$  against  $t$ , where we assume that the enthalpy in supercooled liquid state is independent of thermal history of glass. Figure 3 shows a HRTEM image of as-quenched sample after annealing for  $4.2 \times 10^5$  s at 461 K. Only a maze pattern characteristic to the glass structure is seen and no nanocrystals can be detected. In addition, we examined the change in  $T_x$  (crystallization temperature) and  $\Delta H_x$  (crystallization enthalpy) during the relaxation of the as-quenched sample. The variations in both  $T_x$  and  $\Delta H_x$  with the annealing time were within experimental fluctuations. Thus, we conclude that we can safely rule out the possibility of nanocrystallization during structural relaxation.

In Fig. 4, we compare the change in the specific volume,  $v(t)$ , directly against the change in enthalpy,  $\Delta H_g(t)$ . It can be seen that they are not proportional to each other, and the curve may be divided into two stages. In fact the kinetics shown in Fig. 1 also exhibits two stages, faster kinetics up to  $10^4$  s and slower kinetics thereafter. Thus, it is impossible to explain the kinetics with one-component model, such as the free-volume model. It is well known that the structural relaxation occurs because of many parallel processes, as evidenced by the so-called crossover effect.<sup>3</sup> Our results suggest that at least two components have to be introduced to elucidate the full results.

The free-volume model<sup>12</sup> was initially introduced for a

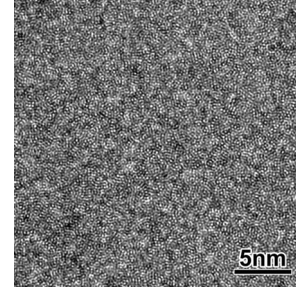


FIG. 3. HRTEM image of the sample relaxed at 461 K for  $4.2 \times 10^5$  s.

system with a hard-sphere potential. When it is applied to metallic alloys, which cannot be adequately described by a hard-sphere potential, the critical volume for atomic diffusion,  $v^*$ , is only about 10% of the atomic volume, rather than about 80% expected for the hard-sphere systems.<sup>12</sup> Cohen and Turnbull, therefore, suggested that in metallic liquids, the free-volume model might apply only for the atomic core, which occupied about 10% of the atom. An alternative model was proposed by Egami *et al.*<sup>16,17</sup> The most prominent change in the pair-density function (PDF) due to structural relaxation is the narrowing of the PDF peaks, including the nearest-neighbor peak, rather than the shifts in their positions.<sup>6</sup> This means that the structural relaxation cannot be explained only by the collapse of the free volume which increases density but requires reduction in both positive and negative density fluctuations. They successfully explained the change in the PDF due to structural relaxation in terms of the narrowing of the distribution of the atomic-level pressure or volume,<sup>18</sup> through annihilation of the  $n$ -type defects (low-density regions, resembling the distributed free volume) and the  $p$ -type defects, (high-density regions, antifree volume).<sup>19</sup> The  $n$ - and  $p$ -type defects are structurally unstable and represent the liquidlike sites.<sup>20</sup> More recently, they<sup>21</sup> suggested that the critical volume strain to define the liquidlike site is  $|\epsilon_v| = 0.11$ , which is close to the estimate by Cohen and Turnbull cited above. In other words, the  $n$ -type defects are characterized by the atomic-level volume strain  $\epsilon_v > 0.11$  while the  $p$ -type defects have  $\epsilon_v < -0.11$ . They also showed that the total concentration of the liquidlike site near  $T_g$  is given by  $p_L = 0.243$ , with the equal concentration for each of the  $n$ -type and  $p$ -type defects.

We analyzed the present results using this model. We assumed that the time-dependent change in the average specific volume of the compressive (high-density or  $p$ -type) region is  $v_c(t)$ , and that of the expansive (low-density or  $n$ -type) re-

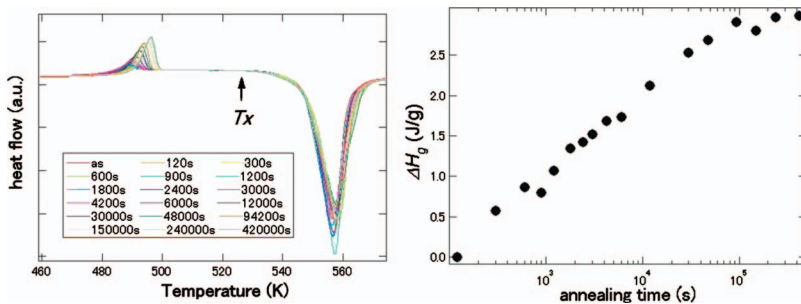


FIG. 2. (Color) (a) The heat-flow curves of  $\text{Pt}_{60}\text{Ni}_{15}\text{P}_{25}$  BMG measured after annealing at 461 K for different times at heating rates of  $0.167 \text{ K s}^{-1}$ . (b) The enthalpy change,  $\Delta H_g(t)$ , as a function of annealing time.

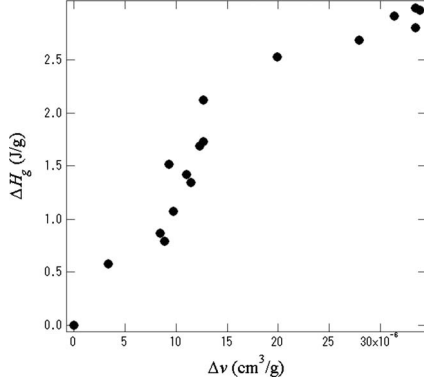


FIG. 4. Direct plot of room-temperature-specific volume change,  $\Delta v(t)$ , against the enthalpy change,  $\Delta H_g(t)$ .

gion is  $v_d(t)$ , where the former expands and the latter shrinks during relaxation. Based on this assumption, the time dependence of the specific volume  $v(t)$  of sample was given as follows:<sup>22</sup>

$$\begin{aligned} v(t) &= p_L[pv_d(t) + (1-p)v_c(t)] + (1-p_L)v_s \\ &= v_{as} + v_d(t) + v_c(t) = v_{as} - p_L p \Delta v_d \{1 - \exp[-(t/\tau_d)^{\beta_d}]\} \\ &\quad - p_L(1-p) \Delta v_c \{1 - \exp[-(t/\tau_c)^{\beta_c}]\} (\Delta v = v_{as} - v_{eq}), \end{aligned} \quad (2)$$

where  $p_L$  is the concentration of liquidlike sites and  $p$  is the fraction of the  $p$ -type (compressive) sites within the liquidlike sites. We assume  $p_L=0.243$  (Ref. 21) and  $p=0.5$ . We also assumed that the ratio,  $\alpha=|v_c(0)/v_d(0)|=|v_c(\infty)/v_d(\infty)|$ , is constant of temperature over the narrow temperature range where measurements were made.

Equation (2) was fitted simultaneously to the data for as-quenched as well as annealed samples. From simulations,  $B_c/B_d \sim 1.5$ , where  $B_c$  and  $B_d$  are the local bulk moduli for the  $p$ -type and  $n$ -type defects.<sup>19</sup> Because the local pressures of the  $p$ -type and  $n$ -type defects,  $p_c$  and  $p_d$ , are similar and opposite in sign,<sup>19</sup> and  $v_c=v_0 p_c/B_c$ ,  $v_d=v_0 p_d/B_d$ , we expect  $\alpha \sim 0.7$ . Indeed, the value of  $\alpha$  obtained by optimal fit, 0.74, is close to the estimated value. Also, even when the value of  $p$  was allowed to vary to improve the fit, it remained very close to 0.5. As shown by solid curves in Fig. 1, Eq. (2) describes the changes in the specific volume calculated from the density experiments quite well for each sample. The parameters are summarized in Table I, and the time dependences of each component,  $v_c(t)$  and  $v_d(t)$ , are shown in Fig. 4.

There are two remarkable features in the result: (a) the both volume changes (expansion and reduction) are much larger than the observed change in the total volume. (b) The relaxation time of the compressed region ( $p$ -type defects) is

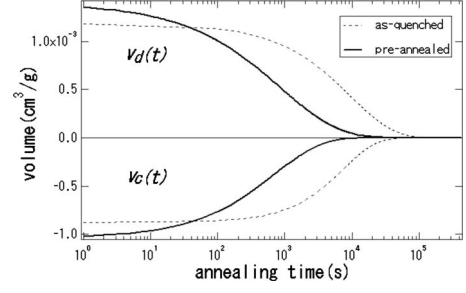


FIG. 5. Changes in volumes,  $v_d(t)$  ( $n$ -type) and  $v_c(t)$  ( $p$ -type), with time at 461 K, with and without preannealing, and they are illustrated as subtracted their initial values. Note that they almost cancel each other, leaving small changes in the total volume.

shorter than that of the expanded region ( $n$ -type defects). The observation (a) is in agreement with the prediction that the structural relaxation occurs by annihilation of the  $n$ - and  $p$ -type defects, and the total volume change is the consequence of the anharmonicity in the interatomic potential.<sup>19</sup> If the interatomic potential is perfectly harmonic,  $\alpha=1$ , the changes in compressed and expanded regions will totally cancel out, and there will be no change in the volume due to the structural relaxation. However, because of the anharmonicity compression is more difficult than expansion, resulting in smaller deviations from the average in the volume of the compressed regions than in the expanded regions.<sup>19</sup> Thus  $\alpha < 1$ , ending up with the net negative change in the total volume. In the free-volume model, on the other hand, compression is impossible because of the hard-sphere potential ( $\alpha=0$ ), thus the volume change is carried totally by the expanded regions (free volume) (Fig. 5).

We also note that the relaxation kinetics of the compressed region is described by the process with Kohlrausch index near 1, meaning that the relaxation kinetics is near Debye type and the distribution of relaxation times is narrow. This is also consistent with the fact that due to steep rise in the repulsive part of the interatomic potential, the distribution in the local atomic volume in the compressed region is small. As a consequence of the observation (b) and Kohlrausch index near 1 for the compressed regions, we see that at the initial stage, both types of defects are annihilated while at the last stage, only the expanded ( $n$ -type) defects are annihilated. This is totally consistent with Fig. 3, which shows that in the initial stage the enthalpy change per volume change is much larger, by a factor of 3–4, than that in the later stage. When two types of defects ( $p$ -type and  $n$ -type) are annihilated the local volume changes cancel each other, leaving a smaller change in total volume. As a consequence, the enthalpy change per total volume change is much larger.

The different kinetics in two regions, compressed and expanded, indicate that  $n$ -type and  $p$ -type defects can annihilate themselves independently, not necessarily through recombina-

TABLE I. Fitting parameters calculated by Eq. (2).

	$\Delta v_{obs}$ (cm <sup>3</sup> /g)	$\Delta v_c$ (cm <sup>3</sup> /g)	$\Delta v_d$ (cm <sup>3</sup> /g)	$\beta_c$	$\beta_d$	$\tau_c$ (s)	$\tau_d$ (s)
As quenched	$3.7 \times 10^{-5}$	$-7.9 \times 10^{-4}$	$1.1 \times 10^{-3}$	0.90	0.68	7494	9409
Preannealed	$4.4 \times 10^{-5}$	$-1.0 \times 10^{-4}$	$1.4 \times 10^{-3}$	0.62	0.52	704	902



nation as defects in semiconductors. Since there is no translational invariance in glasses, the defects can relax locally by emitting long-range stress fields. Our results show that a small change in the fictive temperature results in large difference in the kinetics. We note that the  $\text{Pt}_{60}\text{Ni}_{15}\text{P}_{25}$  BMG is a fragile glass with the fragility  $m=67.2$ ,<sup>7</sup> so that a small change in the fictive temperature can produce large changes in the density of defects.

In Ref. 11, we reported that the kinetics of structural relaxation in a bulk  $\text{Pd}_{40}\text{Ni}_{40}\text{P}_{20}$  glass with annealing up to  $6 \times 10^4$  s at 549 K shows a single relaxation mode. However, this conclusion was based on the linear plot. By plotting the results in logarithmic scale and continuing the annealing up to  $1.2 \times 10^5$  s, we have found that a two-steps relaxation process manifests itself, which is also well described by two-components model. This result leads us to conclude that the structural relaxation of BMGs may be understood, in general, in terms of the two-components model.

Slipenyuk and Eckert experimentally examined the relation between the enthalpy and the volume changes in  $\text{Zr}_{55}\text{Cu}_{30}\text{Ni}_{15}\text{Al}_{10}$  BMG (Ref. 23) during the structural relaxation. Their results indicate  $\Delta H/\Delta v_f \approx 7.58$  kJ/g, where  $\Delta v_f$  is a normalized volume change during relaxation. This value gives 5.89 eV/atom using the molecular weight,  $M_w=74.9$ , of  $\text{Zr}_{55}\text{Cu}_{30}\text{Ni}_{15}\text{Al}_{10}$  glass and is about 2.8 times larger than the formation energy, 2.07 eV/atom,<sup>24</sup> of a single vacancy in a Zr crystal. In the case of the present result,  $\Delta H/\Delta v \approx 140$  kJ/cm<sup>3</sup> = 12.6 eV/atom, is estimated from the initial stage in Fig. 2(b), using  $M_w=133.6$  and the as-cast density,  $d_{as}$ . The formation energies of a single vacancy in the corresponding crystals are reported to be 1.4 and 1.7 eV/atom for Pt and Ni (Ref. 25) atoms. Therefore, the formation energies of free volume per one atomic volume are about 7–9 times larger than those of single vacancies in the crystals. On the other hand, in the two-components model, the volume changes due to the relaxation of the  $n$ - and  $p$ -type defects nearly cancel each other. Consequently, the actual change in volume in absolute value is much larger than the observed change. The actual absolute value of volume change,  $p_L p |\Delta v_d| + p_L (1-p) |\Delta v_c|$  is equal to  $2.3 \times 10^{-4}$  cm<sup>3</sup>/g during the relaxation, and is about six times larger than the total volume change observed,  $|\Delta v_{obs}| = 3.7 \times 10^{-5}$  cm<sup>3</sup>/g, as indi-

cated in Table I. As a consequence, the formation energy of free volume is reduced to  $12.6/6 \approx 2.1$  eV/atom and it is of the similar magnitude with the formation energy of a single vacancy in the crystal. Whereas the kinematical behavior of enthalpy during relaxation in Fig. 2(b) may appear to be describable by a single-component model rather than the two-components model, this result is also compatible with the two-components model because the change in enthalpy due to annihilation of both the  $n$ - and the  $p$ -type defects results in positive heat release. As a result, the net relaxation curve is the superposition of two stretched exponential relaxation curves, with slightly different  $\tau$  and  $\beta$  values, and appears as a single stretched exponential function. In Fig. 1, we also show the fit with a single stretched exponential relaxation function, in addition to the fit with the two-components model. Obviously, the single-component curve is not in an agreement with the data.

We note that the relaxation process includes, in general, the chemical short-range ordering (CSRO) process<sup>5,26</sup> as well as the topological short-range ordering (TSRO) process, and the present data may reflect some of the CSRO process. However, the coupling of the CSRO to volume is relatively weak,<sup>27</sup> and usually faster than the TSRO relaxation.<sup>26,27</sup> Also generally the CSRO relaxation occurs over the temperature range significantly below  $T_g$ .<sup>26,27</sup> Because the present study of volume and enthalpy relaxation was carried out in the close vicinity of the glass transition, we conclude that the effect of the CSRO relaxation is negligible.

In conclusion, we have shown through careful measurements of changes in volume and enthalpy that the structural relaxation in  $\text{Pt}_{60}\text{Ni}_{15}\text{P}_{25}$  BMG cannot be described by a single-component model, such as the traditional free-volume model but requires at least two components. We suggest that the local-density-fluctuation model involving both high- and low-density regions can satisfactorily elucidate the results.

We would like to appreciate H. S. Chen for supplying appropriate suggestions on the mechanism of structural relaxation. The research at the University of Tennessee and Oak Ridge National Laboratory was supported by the Division of Materials Sciences and Engineering, Office of Basic Energy Sciences, U.S. Department of Energy under Contract No. DE-AC05-00OR-22725 with UT-Battelle.

<sup>1</sup>A. Inoue *et al.*, Mater. Trans., JIM **31**, 425 (1990).

<sup>2</sup>A. Peker and W. L. Johnson, Appl. Phys. Lett. **63**, 2342 (1993).

<sup>3</sup>For example, G. W. Scherer, *Relaxation in Glasses and Composites* (Wiley, New York, 1986).

<sup>4</sup>H. S. Chen, Rep. Prog. Phys. **43**, 353 (1980).

<sup>5</sup>T. Egami, Ann. N. Y. Acad. Sci. **37**, 238 (1981).

<sup>6</sup>T. Egami, J. Mater. Sci. **13**, 2587 (1978).

<sup>7</sup>H. Kato *et al.*, Scr. Mater. **54**, 2023 (2006).

<sup>8</sup>R. Busch *et al.*, Acta Mater. **46**, 4725 (1998).

<sup>9</sup>J. F. Wang *et al.*, J. Phys. D **38**, 946 (2005).

<sup>10</sup>I. Gallino *et al.*, Acta Mater. **55**, 1367 (2007).

<sup>11</sup>O. Haruyama and A. Inoue, Appl. Phys. Lett. **88**, 131906 (2006).

<sup>12</sup>M. H. Cohen and D. Turnbull, J. Chem. Phys. **31**, 1164 (1959).

<sup>13</sup>A. J. Kovacs *et al.*, J. Phys. Chem. **67**, 152 (1963).

<sup>14</sup>F. Spaepen, Acta Metall. **25**, 407 (1977).

<sup>15</sup>F. Faupel *et al.*, Rev. Mod. Phys. **75**, 237 (2003).

<sup>16</sup>T. Egami *et al.*, Philos. Mag. A **41**, 883 (1980).

<sup>17</sup>T. Egami and D. Srolovitz, J. Phys. F: Met. Phys. **12**, 2141 (1982).

<sup>18</sup>D. Srolovitz *et al.*, Phys. Rev. B **24**, 6936 (1981).

<sup>19</sup>T. Egami *et al.*, J. Phys. (France) **41**, C8–272 (1980).

<sup>20</sup>M. H. Cohen and G. S. Grest, Phys. Rev. B **20**, 1077 (1979).

<sup>21</sup>T. Egami *et al.*, Phys. Rev. B **76**, 024203 (2007).

<sup>22</sup>O. Haruyama *et al.*, J. Phys.: Conf. Ser. **144**, 012050 (2009).

<sup>23</sup>A. Slipenyuk and J. Eckert, Scr. Mater. **50**, 39 (2004).

<sup>24</sup>O. Le Bacq *et al.*, Phys. Rev. B **59**, 8508 (1999).

<sup>25</sup>P. A. Korzhavyi *et al.*, Phys. Rev. B **59**, 11693 (1999).

<sup>26</sup>T. Egami, Mater. Res. Bull. **13**, 557 (1978).

<sup>27</sup>B. Porscha and H. Neuhäuser, Scr. Mater. **32**, 931 (1995).